MICROSTRUCTURE-SENSITIVE ICME WORKFLOWS FOR FATIGUE CRITICAL APPLICATIONS

Krzysztof S. Stopka[1], Gary Whelan[2], and David L. McDowell[1,2]

[1] Woodruff School of Mechanical Engineering, [2] School of Materials Science and Engineering
Georgia Institute of Technology, Atlanta, GA 30332-0405, USA

ABSTRACT

Fatigue cracks form and grow in fatigue critical structural alloys that are relevant to Naval aviation applications from nucleant grains, phases, or constituent particles in the high cycle fatigue (HCF) regime. To enable progress in configuring Integrated Computational Materials Engineering (ICME) towards addressing improved fleet performance, we present a multilevel scripted ICME workflow that employs microstructure-sensitive simulations. An inductive design exploration framework considers various sources of uncertainty to inform robust decisions regarding materials development necessary to achieve desired performance of fatigue critical components, given accessible process paths and resulting microstructures. Uncertainty propagation through model chains (whether models are surrogates, empirical, or based on simulation) is considered. Digital statistical volume element representations of microstructure are employed, with structure-property relations based on microstructure-sensitive computational fatigue modeling using the crystal plasticity finite element method, addressing sensitivity to microstructure resulting from process path including both intrinsic (grain/phase size, shape and orientation distributions) and extrinsic (residual stresses, surface roughness, nonmetallic inclusions or pores) features. The digital workflow considers extreme value (minimum property) fatigue response as the primary performance requirement. The framework is exercised to explore available microstructures for α-β Ti-6Al-4V. The work has potential to impact development of new and improved fatigue critical material systems relevant to naval applications.

1. INTRODUCTION

Fatigue failure is of utmost concern in design of industrial components, and its cost is estimated to account for as much as 4 % of the gross national product [1]. While extensive experimental testing has been performed to gain insight into the mechanisms of fatigue crack formation and growth, modern testing and characterization techniques have outpaced the ability to fully understand information gathered from such experiments [2]. Massive experimental datasets contain stress- and strain-life information that ostensibly support the design of components, but understanding of the underlying physical mechanisms driving fatigue failures is deficient, relations to microstructure are tenuous, and the translation of fatigue concepts and test data to design engineering is incomplete. Design engineers and failure analysts still often rely on empirical correlations to deal with surface roughness, residual and mean stresses, combined stress state effects, and corrosion. Additionally, the high degree of data scatter in the HCF regime often requires high safety factors, resulting in excess weight.

Copyright 2019. Used by the Society of the Advancement of Material and Process Engineering with permission.

SAMPE Conference Proceedings. Charlotte, NC, May 20-23, 2019. Society for the Advancement of Material and Process Engineering – North America.

While standard fatigue experiments are essential to validate and calibrate numerical models, they are inherently limited; the complex cause-and-effect interactions between grains/phases, secondary particles and other long-range interactions often remain elusive. Synchrotron diffraction and tomography experiments may assist in this regard, but are of high cost and limited sample size. Fatigue experiments are time-intensive and often require a number of samples due to the high degree of variability. Different specimen, loading, and environment conditions quickly exacerbate cost. ICME leverages the growing capability of computational resources to augment experiments with numerical simulations of response of material microstructures to provide additional decision support in materials selection and design processes [3]. These numerical studies leverage 3D digital microstructures that attempt to mimic actual microstructures, facilitating detailed analysis of stress, strain and other parameters that are related to fatigue mechanisms at the scale of microstructure. Digital workflows to generate and explore the material response of the digital microstructures are scripted in the Python open-source software and utilize crystal plasticity finite element method (CPFEM) models with ABAQUS [4].

Over the last decade, this kind of ICME workflow has advanced the capability to rank order fatigue resistance among accessible microstructures forces for a variety of materials, corresponding microstructure attributes, and loading conditions. Specific examples include Ni-based superalloy IN100 [5-10], martensitic gear steels [11, 12], airframe aluminum alloys [13-16], and titanium alloy Ti-6Al-4V [17, 18]. Nevertheless, several technological gaps remain to be addressed, such as explicit representation and effects of surface roughness, residual stresses, pores/inclusions, and other pre-existing defects, as well as consideration of multiaxial loading conditions. Pursuit of robust decision support for fatigue critical applications that reflect these effects is vital for future naval applications.

2. METHODOLOGY

ICME is realized in the context of exploring fatigue criticality by decomposing the material process-structure-property-performance (PSPP) linkages. Process-structure (PS) linkages describe how process route affects material microstructure, and are often constructed empirically using expert guidance and/or available experimental results. On the other hand, structure-property (SP) linkages can be systematically explored using microstructure-sensitive computational models to augment experimental information. Digital representation of microstructures along with the application of computational models allows for the study of property variation associated with microstructure, surface conditions, and residual stresses obtained via different processing routes. CPFEM models estimate material responses of these digital microstructures under various loading conditions. Fatigue Indicator Parameters (FIPs) serve as surrogate measures for driving forces for fatigue crack formation and early growth. FIPs are computable Quantities of Interest (QoIs) used to explore the fatigue criticality of various combinations of material microstructures and loading conditions, subject to uncertainty. The FIPs are fit to known Extreme Value Distributions (EVD) to aid in the analysis of rare event (extreme value) failure modes such as fatigue. Uncertainty quantification and propagation through the digital workflows are explicitly addressed.

2.1 Process-Structure-Property Linkages

Traditional materials science and engineering practice has tended to focus on reductionism, rather than a systems approach. With the recent advances in computational tools in this area, the science of materials can radically shift in terms of the way materials are considered in the design process.

By considering the structure of the material as part of the design process rather than simply selecting from a list of available materials, the component level performance can be improved. One of the major impediments to this vision is the difficulty of communicating the complexities of the hierarchy of length scales and microstructure features that control variability of material responses to the design process, using digital structure information, computational tools, and physical experimentation [19].

In design engineering, quality function deployment (QFD) tools are used to call attention to the customer needs. These QFD tools provide a structured approach to define customer requirements and translate them to engineers in the form of engineering attributes. A PSPP map is an analogous system design chart that can be used in the material design process so that materials engineers can clearly see the important linkages that influence the material system to facilitate design of the material for specific application requirements [20]. Figure 1 provides an example of a PSPP map developed for Ti-6Al-4V for application as an aerospace alloy. The performance column lists structural component attributes to be addressed in design for a particular application, while the property column provides the measurable properties relating to these performance requirements. The PS linkages represent material structures as affected by available processing routes. A fleshed-out structure space therefore facilitates design exploration across the space of accessible material structures and properties.

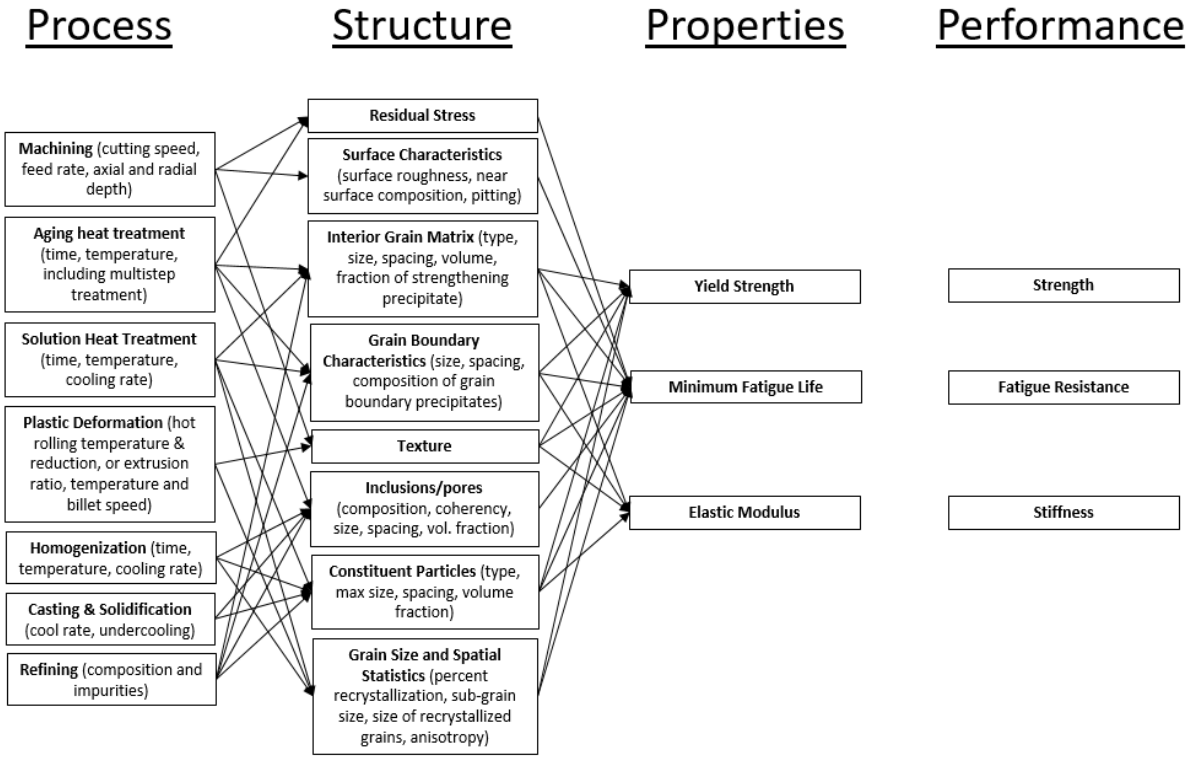


Figure 1. Ti-6Al-4V PSPP map [21].

2.2 Representation of Microstructure

Probabilistic modeling of rare event (extreme value) failure processes such as fatigue is greatly affected by the inputs used in the microstructure-sensitive computational models employed. Both intrinsic (grain/phase size and shape, orientation) and extrinsic (surface roughness, residual stresses, non-metallic inclusions and pores, etc.) features can vary. The ability to accurately model these features allows for the realistic exploration of their effects in comparing fatigue criticality of various accessible microstructures for materials of interest.

The discretized microstructures employed here are generated using the open source Dream.3D software [22], which allows for a versatile, robust and consistent modeling environment, as well as the opportunity for others to explore similar materials science inquiries [23]. An example of one such instantiation is shown below in Figure 2, in which colors indicate different grains of duplex α-β Ti-6Al-4V. Dream.3D also has the ability to generate microstructures using experimentally obtained data, such as EBSD [24, 25].

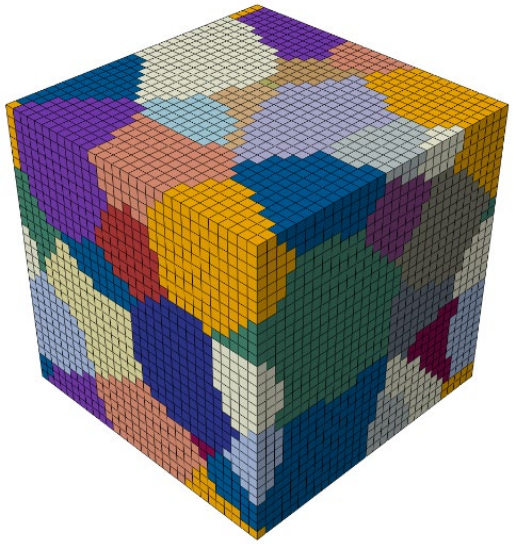


Figure 2. Sample microstructure instantiation generated with Dream.3D [22] with different colors indicating different grains.

Typical CPFEM model outputs include stress, strain, and inelastic strain at every element in the discretized microstructure. Macroscopic properties such as elastic stiffness and yield strength can be estimated by considering the volume averaged stress-strain response. Although average stress-strain behavior or elastic stiffness may require representative volume elements (RVE) that are relatively small in terms of number of included grains or phases, the RVE concept is not as useful for fatigue crack formation due to its rare-event nature [26, 27]; a RVE would be untenably large for computation. For this reason, sampling of ensembles of microstructure samples, so-called Statistical Volume Elements (SVEs), is employed to compute statistical distribution of responses. These SVE ensembles are generated based on predefined distributions of key microstructure attributes [28, 29]. Representation of extrinsic features such as surface roughness, or long range and short range residual stress introduces additional complexity [10], with material- and process-specific dependencies.

2.3 Modeling of Materials

The exploration of SP linkages utilizes crystal plasticity microstructure-sensitive computational models that consider slip system level dislocation behavior specific to each crystal structure and alloy system of interest. Using the previously described Dream.3D microstructures as inputs, ranged sets of loading and boundary conditions may be specified to investigate various material responses. The models utilize a rate-sensitive flow rule and associated hardening rules to simulate individual slip system activity, and are implemented into finite element simulations as User MATerial (UMAT) subroutines in ABAQUS [13, 30-32].

2.4 Evaluation of Fatigue Criticality

Traditional strain- and stress-life fatigue correlations do not explicitly address material microstructure, serving as purely empirical correlations. Microstructure-sensitive CPFEM simulations take a more physically based approach by considering how material structure affects fatigue resistance via computation of distributions of FIPs. The formulation of FIPs have built on foundations of advanced methods based on strain, stress and energy methods developed to address shortcomings of empirical approaches and address multiaxial loading conditions [33]. Brown and Miller [34] proposed that a combination of tensile strain and plastic shear strain on a critical plane should be used to correlate transgranular fatigue crack formation and growth in alloys. Fatemi and Socie [35] built on this critical plane concept to augment dependence on the cyclic plastic shear strain with the peak tensile stress normal to the plane of maximum shear strain range. For a specified length of initiated fatigue crack, the correlation between critical plane parameter and the number of cycles to form a crack is expressed as

$$f(\mathrm{N}) = \frac{\Delta\gamma^{\mathrm{p}}_{\mathrm{max}}}{2}\left[1 + \mathrm{k}^{*}\frac{\sigma^{\mathrm{max}}_{\mathrm{n}}}{\sigma_{\mathrm{y}}}\right] = \mathrm{FIP}_{\mathrm{FS}} \qquad [1]$$

where $f(\mathrm{N})$ is a constant for a given number of cycles to form a crack of specified length, $\Delta\gamma^{p}_{max}$ is the maximum plastic shear strain range, σ_n^{max} is the peak stress normal to the plane of maximum plastic shear strain range, σ_y is the macroscopic yield strength of the material, and k^* is a constant which controls the influence of the normal stress. In this work, FIPs are computed throughout the microstructure. The form of the Fatemi-Socie FIP (FIP_{FS}) in equation 1 correlates well with experimental findings for multiaxial fatigue across a range of strain states [36]. McDowell and Berard [37] showed that the FIP_{FS} can be related to the ΔJ-Integral of elastic-plastic fracture mechanics (EPFM), which has been used to correlate the rate of microcrack propagation. Castelluccio and McDowell further demonstrated [38] that the FIP_{FS} correlates well with the crack tip displacement range (ΔCTD) for cracks in homogeneous single crystals or cracks along the interface of slip bands and matrix in single crystals, suggesting utility of its use as a surrogate driving force measure for the formation and growth of microstructurally small fatigue cracks. While FIP_{FS} is intended to correlate with transgranular fatigue crack formation (left of Figure 3), the Grain Boundary Impingement FIP (FIP_{GBI}) captures the accumulation of net plastic strain at grain boundaries which leads to intergranular fatigue crack formation and growth (right of Figure 3), and is shown below as equation 2, where γ^{p}_{net} is the net plastic shear strain at the grain/phase boundary, σ_n^{max} is the averaged stress normal to the grain boundary, σ_y is the macroscopic yield strength, and k_n is a scaling parameter. Many other types of FIPs can be defined; several reviews detailed the methodology behind the use of FIPs for modeling fatigue crack formation [39, 40].

$$\frac{\gamma_{net}^{p}}{2}\left[1+k_n\frac{\sigma_n^{max}}{\sigma_y}\right]=FIP_{GBI} \quad [2]$$

Fatigue crack formation occurs over some finite damage process zone, and therefore the calculated FIPs must be averaged over an appropriate volume; this also regularizes the solution and mitigates mesh sensitivity. The averaging volume should be held fixed over a given set of simulations intended to compare fatigue resistance among microstructures. Averaging of the entire grain volume is unsuitable since it smears out local high values of FIPs within grains; moreover, the grain size has a distribution. More advanced formulations have been developed recently which split grains into bands representative of the material's crystallographic slip systems [41]. FIPs may be averaged over these bands or over smaller regions in the bands to achieve a consistent averaging volume.

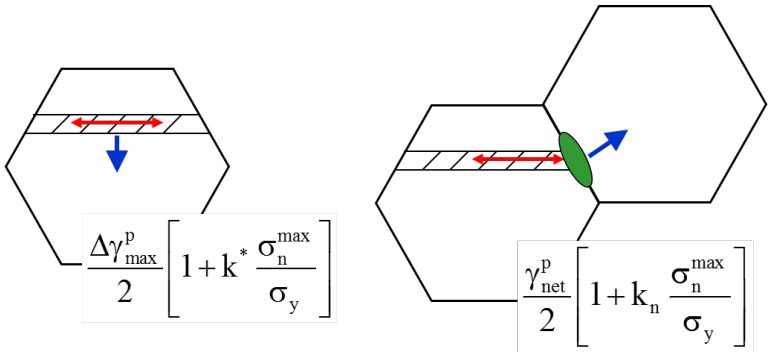


Figure 3. Representations of the Fatemi-Socie (left) and Grain Boundary Impingement (right) FIP.

To properly represent statistic distributions of potential sites for fatigue crack formation, we generate ensembles of SVEs and execute CPFEM simulations in which cyclic straining is applied to the point of elastic-plastic shakedown. The FIP_{FS} is computed at every element within the digital microstructures, after which volumetric averaging is performed. Afterwards, the highest FIP from each SVE is extracted or the extreme value distributions of FIPs are extracted regardless of origin. These are fit to known EVDs so that trends of FIPs from SVE ensembles of different microstructures may be compared to one another. Conclusions may then be drawn regarding relative fatigue resistance between sets of microstructures. One application of this process involved the rank-ordering of different microstructures of duplex Ti-6Al-4V by Przybyla and McDowell [17]. Ensembles of 100 SVE instantiations of four different microstructure variants were subjected to cyclic straining at 0.6 %. Grain-averaged values of FIP_{FS} were calculated for each SVE and fit to a Gumbel EVD. The microstructures with larger grains and higher percentage volume fraction of alpha phase exhibited the highest FIPs (and therefore the highest driving forces to form fatigue cracks), which agrees well with experimental findings of similar titanium alloys [42]. A similar computational study was recently performed as part of this work in which several microstructure variants of Ti-6Al-4V were explored. The previously mentioned study examined SVE ensembles varying in grain size and composition, while the recent work explored the effects of different textures on fatigue resistance. Four different textures of Ti-6Al-4V were subjected to completely reversed cyclic straining at 0.6 %, inspired from literature and previous work [31, 43, 44]. The <0001> pole figures are shown below in Figure 4. Uniaxial straining was in the x-direction, representative of the left-right directions on the pole figures.

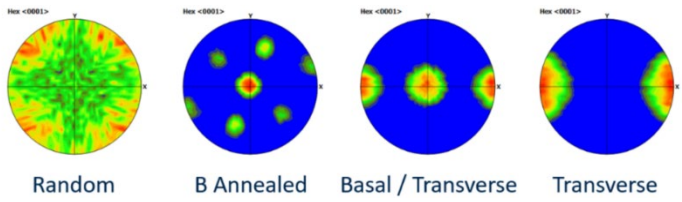


Figure 4. Textures used in the Ti-6Al-4V microstructure-sensitive texture study.

Three fully reversed computational cycles were applied for stress-strain shakedown, after which the FIP_{FS} was calculated and averaged over regions within the bands of the grains. The location of the highest FIP was chosen as the site of fatigue crack formation (i.e., nucleant grain), and these elements were computationally "damaged"; this formulation significantly reduces the stiffness tensor of damaged elements when the stress normal to those elements is tensile and is performed in an isotropic manner. The stiffness is restored when the stress normal to the plane of these elements becomes compressive, which emulates a crack closure effect. The SVEs then underwent another three loading cycles to allow for complex stress-strain redistribution [41]. Afterwards, the FIP_{FS} were recomputed, and these two sets of FIPs (before and after a crack was introduced into the microstructures) were compared to assess the effects of an explicit fatigue crack on FIP distributions. Figure 5 shows one such example of the computed uncracked vs. cracked FIPs (in blue and red markers, respectively) to examine the effect of texture on fatigue crack formation driving forces; the x-axis represents FIP magnitude and the y-axis represents probability. The probability p is linearized and a true extreme value Gumbel distribution appears as a straight line [6]. In Figure 5, FIPs are sorted in ascending order and different markers indicate texture. Considering first the uncracked FIP datasets (blue data markers), the basal-transverse textured FIPs are lowest in magnitude, while random and transverse textured FIPs are highest depending on probability. Fatigue is an extreme value event, and so the FIPs of highest magnitude are of interest. Although at low probability the random textured FIPs are highest in magnitude, at high probability the transverse textured FIPs are highest in magnitude, while random textured FIPs are second highest. This indicates that for the specific loading conditions, the basal-transverse and transverse textured SVEs are most and least resistant to initial fatigue crack formation within the nucleant grain, respectively.

The FIP_{FS} values are recalculated following several cycles of stress-strain redistribution after crack formation. In this compilation of cracked FIPs, the nucleant grain is no longer sampled; this sampling technique pertains to fatigue crack formation driving forces in other grains throughout each SVE. While it is simple to rank order different textures based on their initial (uncracked) FIP datasets, comparison of uncracked vs. cracked FIPs for a single texture is non-trivial. Therefore, a systematic way to evaluate uncracked vs. cracked FIP trends between different textures is to consider the average percentage change between some of the higher FIP_{FS} values. Figure 6 presents this information, and its interpretation is as follows: when comparing the basal-transverse FIPs, the highest 20 cracked FIPs decrease by an average of 45 % in magnitude when compared to uncracked FIPs. Similarly, the five highest random textured FIPs decrease on average by only 5 % in FIP magnitude when comparing cracked and uncracked FIPs. This Figure indicates that the basal-transverse and random textured FIPs exhibit the highest and lowest decrease in FIP magnitude, respectively. Therefore, upon introduction of a fatigue crack into the SVEs and subsequent stress-strain redistribution, the basal-transverse texture exhibits the best relative resistance to further fatigue crack formation in other grains in the SVE.

In summary, the basal-transverse FIPs are not only of lowest magnitude in terms of initial fatigue crack formation driving forces, but they are also highest in decrease (relative to the other textures considered) in terms of further fatigue crack formation driving forces in other grains. Conversely, there is clear competition between the transverse and random textured FIPs in terms of uncracked FIP magnitude and smallest decrease in further fatigue crack formation driving forces. This may indicate increased resistance to fatigue crack formation and growth for basal-transverse textured components in the loading conditions considered here (uniaxial completely reversed cyclic straining at 0.6% in the left-right direction relative to ODF pole figures). The example presented here is just one application of the ICME workflow for microstructure-sensitive fatigue assessment to compare fatigue resistance among various accessible microstructures in a given alloy system.

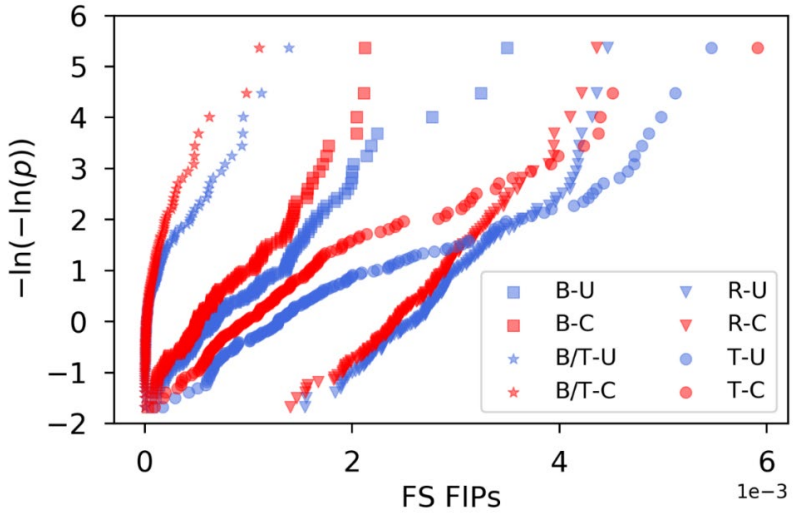


Figure 5. Fatemi-Socie FIPs (FIP_{FS}) fit to the Gumbel EVD for duplex Ti-6Al-4V at 0.6 % max-applied strain. Texture legend key: “B”: beta-annealed, “B/T”: basal-transverse, “R”: random, “T”: transverse, “U”: uncracked FIPs marked in blue, “C”: cracked FIPs marked in red.

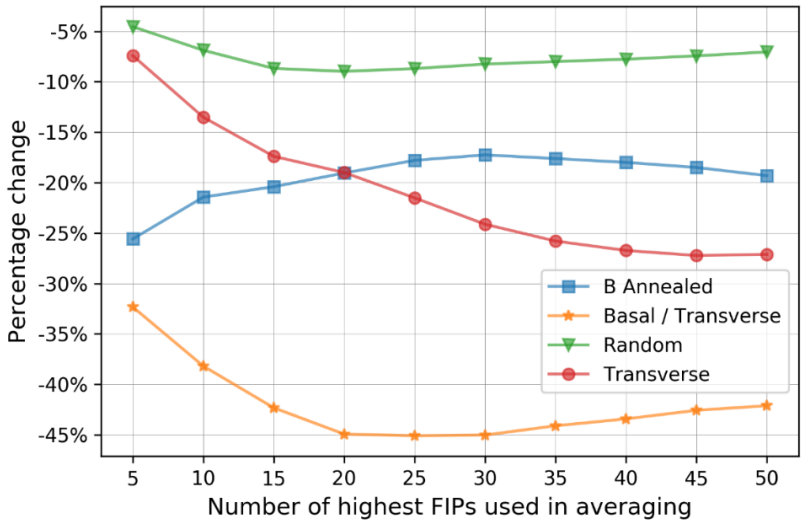


Figure 6. Uncracked vs. cracked FIP percentage changes for duplex Ti-6Al-4V at 0.6 % max-applied strain.

2.5 Uncertainty Quantification and Propagation

With the goal of exploring fatigue criticality of engineering alloys, decision-making can be better informed when uncertainty is measured and propagated through the various steps in the workflow. Robust design has gained widespread attention in ICME with applications in reliable decision making for complex engineering systems [45], seeking solutions that are relatively insensitive to small changes in uncertain quantities [46]. IDEM is an attractive approach for robust design as it provides a computational workflow for generating robust design decision support in the face of uncertainty [47]. However, the existing uncertainty quantification protocols included in the pyDEM computational environment [48] can be updated as desired to reflect various state-of-the-art UQ methodologies. Both the inherent, irreducible (i.e., aleatory) uncertainty in the system (quantified as statistical distributions) and uncertainty that can be reduced by increasing the knowledge of the system (i.e., epistemic) should be considered.

In the interest of quantifying uncertainty it is important to first identify the QoIs for which uncertainty is to be quantified, in this case the computed FIPs. **Microstructure statistics uncertainty** (MSU) is the inherent uncertainty in the quantification of the various microstructure attributes resulting from natural stochasticity in microstructures that originates from the PS linkages and, once quantified, must be propagated through SP linkages to determine uncertainty in QoIs.

Model form uncertainty (MFU) is a combination of the uncertainty associated with the formulation of the constitutive model as well as the nature of the computational model (e.g., boundary conditions), and the number and size of SVEs used to compute distributions of FIPs. **Model parameter uncertainty** (MPU) is the uncertainty resulting from limitation in calibrating parameters in the model based on the amount of data available. For example, if a constitutive model is only calibrated with one cyclic stress-strain dataset having a specific strain amplitude, ratio, and rate, as well as one set of microstructure statistics, the model parameters selected may fit well to this data but perform less adequately with a different design of experiment.

To demonstrate the effect of MSU on the QoIs in Ti-6Al-4V, nominal feasible values were assigned to the volume fraction of primary alpha phase (0.3), average grain size (30 μm), and crystallographic texture (basal-transverse) as the microstructure attributes of interest. The uncertainty in each microstructure attribute was estimated by examining existing literature for ranges of realized microstructure statistics for given nominal microstructures, and then Gaussian distributions were assigned to each, with average values assigned to desired nominal values. Figure 7 shows the probability density functions (PDFs) for average grain size (top left) [49] and volume fraction of primary alpha phase (top right) [50], as well as the <0001> pole figures for the nominal basal-transverse texture with one standard deviation variation in intensity [51]. The CPFEM simulations conducted to propagate uncertainty in the microstructure statistics to the FIP_{FS} response contained 20 SVEs, and were cycled to a peak strain of 0.6 % at a strain ratio (min/max) of -1 and a strain rate of 0.001 s^{-1}. Three uniaxial, fully reversed cycles were applied in x-direction with periodic boundary conditions. A lognormal grain size distribution of 30 μm ± 7.5 μm resulted in approximately 90 grains per SVE. The results are shown in Figure 8 and Figure 9.

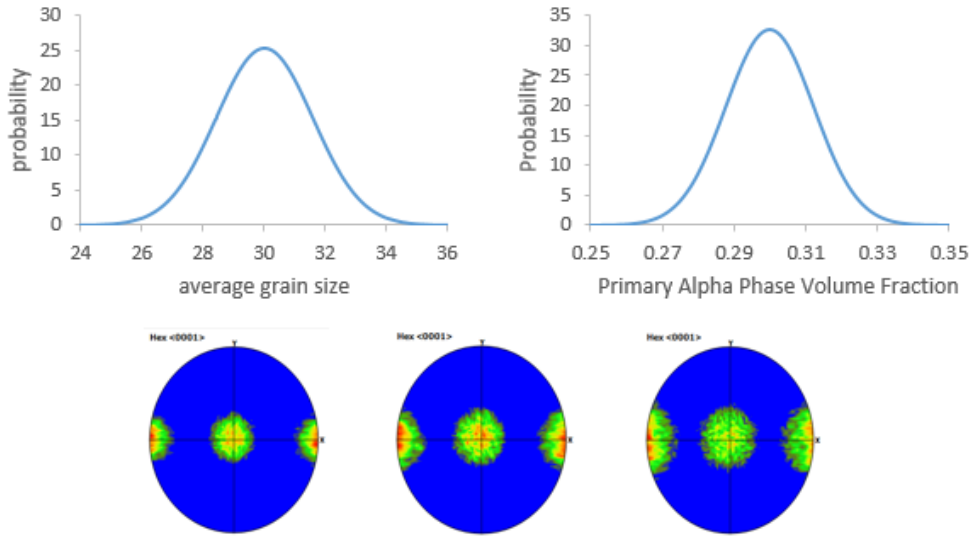


Figure 7. Statistical distributions of microstructure attributes for Ti-6Al-4V with nominal grain size of 30 μm (top left), volume fraction of primary alpha phase of 0.30 (top right), and basal-transverse texture with varied intensity (bottom).

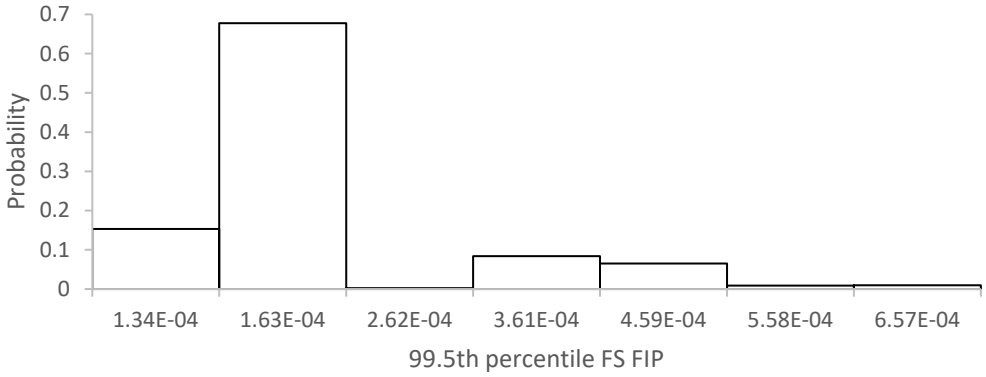


Figure 8. Output histograms of 99.5th percentile FS FIPs for Ti-6Al-4V.

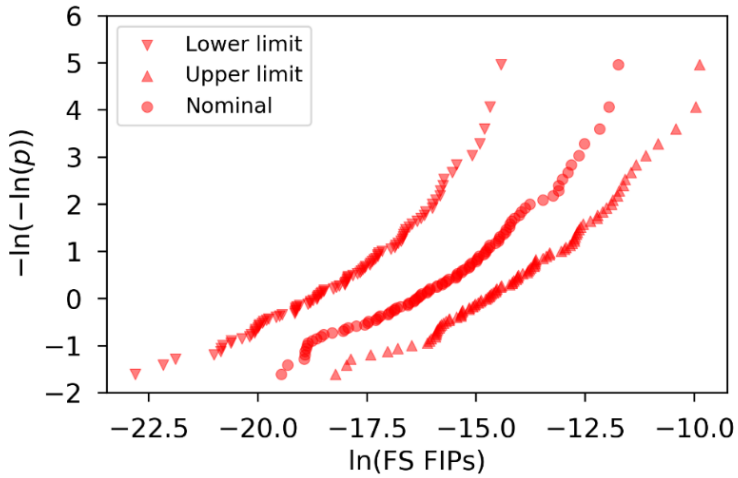


Figure 9. FIP_{FS} response for nominal Ti-6Al-4V microstructure and the upper and lower limits of 99.5^{th} percentile FIP_{FS} values plotted on a Fréchet distribution.

Figure 8 shows the histogram of the resulting distribution of 99.5th percentile FIP_{FS} for this microstructure amongst the full ensemble of SVEs. Figure 9 shows the nominal FIP_{FS} plotted using coordinates corresponding to a Fréchet distribution, as well as the maximum and minimum FIP_{FS} response occurring within two standard deviations of the nominal microstructure statistics. The "lower limit" corresponds to the FIP_{FS} response from the sample microstructure dataset that had the lowest 99.5th percentile FIP_{FS}. This occurred when primary alpha phase volume fraction, average grain size, and texture intensity are two, two, and one standard deviations below average, respectively. The probability of a microstructure occurring with these statistics is approximately 0.01 %. Similarly, the "upper limit" is the FIP_{FS} response from the sample microstructures have two, two, and one standard deviation above average.

These results demonstrate that the uncertainty in considering just these three microstructure attributes has a significant impact on the predicted FIP_{FS} response, with a range in FIP_{FS} values of approximately half an order of magnitude for the same nominal microstructure. Additionally, the shape of the histogram demonstrates that the resulting uncertainty can have a non-trivial distribution that would be difficult to predict without propagating uncertainty through the CPFEM model or an adequate surrogate model. Due to the significant computational cost of these simulations, the surrogate modeling approach would be necessary to explore the design space.

The relative sensitivity was much lower for primary alpha phase volume fraction and average grain size compared with texture. This implies that for robust design, a materials manufacturer should focus more resources on uncertainty reduction for the crystallographic texture than on other microstructure attributes for Ti-6Al-4V. Similarly, surrogate models used to explore design space should be trained more thoroughly in these higher sensitivity regions. Additionally, the results imply that a nominal microstructure that achieves the performance of interest without relying on a basal-transverse texture would be more robust, as the basal-transverse texture results in the lowest FIP_{FS} response of all common Ti-6Al-4V textures as previously shown in Figure 5. For example, if other microstructure attributes having a lower degree of uncertainty associated with them could be tuned to achieve the necessary FIP_{FS} response whilst the crystallographic texture is kept random, then the upper limit of FIP_{FS} response from a nominal basal-transverse texture would provide a robust design. Lastly, the statistical representation of this uncertainty, as opposed to simple error bounds, allows for precise understanding of the degree of reliability of a given design and decisions can be made accordingly. This uncertainty informed design decision support process can be systematically carried out by integrating the current uncertainty quantification and propagation workflows into the pyDEM environment.

Moving forward, the same uncertainty quantification and propagation methodology can be extended to the remainder of the SP linkages outlined in Figure 1 as well as those for other material systems. This will facilitate robust uncertainty informed decision support for both intrinsic (grain/phase size, shape and orientation distributions) and extrinsic (residual stresses, surface roughness, nonmetallic inclusions or pores) features.

3. CONCLUSIONS

To accelerate the rate at which materials are designed for components critical to future naval applications, multilevel scripted computational workflows utilize microstructure-sensitive computational models to explore material behavior. Digital representations of materials capture intrinsic and extrinsic variations to microstructure. These undergo deformation using CPFEM models to determine material behavior from which FIPs can be analyzed to determine fatigue response. Consideration of uncertainty quantification and propagation facilitates robust decision support.

A previous application of ICME specific to grain size and composition of duplex α-β Ti-6Al-4V was reviewed, and in the case study explored, crystallographic texture variants of this material were ranked-ordered by their resistance to fatigue crack formation. Specifically, the basal-transverse texture exhibited the highest resistance to fatigue crack formation, whereas the transverse and random textured microstructures competed as lowest. Several remaining key technological gaps (modeling of residual stresses, surface roughness, pores/inclusions, and other pre-existing defects, as well as multiaxial loading conditions) are being addressed as part of this work.

4. ACKNOWLEDGEMENTS

This work was sponsored by the Office of Naval Research (ONR), under grant number N00014-17-1-2036. The views and conclusions contained herein are those of the authors only and should not be interpreted as representing those of ONR, the U.S. Navy or the U.S. Government.

5. REFERENCES

[1] R. I. Stephens, A. Fatemi, R. R. Stephens, and H. O. Fuchs, Metal fatigue in engineering. John Wiley & Sons, 2000.

[2] D. L. McDowell, "Basic issues in the mechanics of high cycle metal fatigue", *International Journal of Fracture,* 80 (1996) 103-145. https://doi.org/10.1007/bf00012666

[3] J. H. Panchal, S. R. Kalidindi, and D. L. Mcdowell, "Key computational modeling issues in integrated computational materials engineering", *Computer Aided Design,* 45 (1) (2013) 4-25. https://doi.org/10.1016/j.cad.2012.06.006

[4] Abaqus (2017) https://www.3ds.com/products-services/simulia/products/abaqus/ (accessed April 18, 2017).

[5] W. D. Musinski and D. L. McDowell, "Microstructure-sensitive probabilistic modeling of hcf crack initiation and early crack growth in ni-base superalloy in100 notched components", *International Journal of Fatigue,* 37 (2012) 41-53. https://doi.org/10.1016/j.ijfatigue.2011.09.014

[6] C. P. Przybyla and D. L. McDowell, "Microstructure-sensitive extreme value probabilities for high cycle fatigue of ni-base superalloy in100", *International Journal of Plasticity,* 26 (3) (2010) 372-394. http://doi.org/10.1016/j.ijplas.2009.08.001

[7] M. Shenoy, J. Zhang, and D. L. McDowell, "Estimating fatigue sensitivity to polycrystalline ni-base superalloy microstructures using a computational approach", *Fatigue & Fracture of Engineering Materials & Structures,* 30 (10) (2007) 889-904. https://doi.org/10.1111/j.1460-2695.2007.01159.x

[8] N. Salajegheh and D. L. McDowell, "Microstructure-sensitive weighted probability approach for modeling surface to bulk transition of high cycle fatigue failures dominated by primary inclusions", *International Journal of Fatigue,* 59 (2014) 188-199. https://doi.org/10.1016/j.ijfatigue.2013.08.025

[9] W. D. Musinski and D. L. McDowell, "Simulating the effect of grain boundaries on microstructurally small fatigue crack growth from a focused ion beam notch through a three-dimensional array of grains", *Acta Materialia,* 112 (2016) 20-39. https://doi.org/10.1016/j.actamat.2016.04.006

[10] W. D. Musinski and D. L. McDowell, "On the eigenstrain application of shot-peened residual stresses within a crystal plasticity framework: Application to ni-base superalloy specimens", *International Journal of Mechanical Sciences,* 100 (2015) 195-208. https://doi.org/10.1016/j.ijmecsci.2015.06.020

[11] R. Prasannavenkatesan, J. Zhang, D. L. McDowell, G. B. Olson, and H.-J. Jou, "3d modeling of subsurface fatigue crack nucleation potency of primary inclusions in heat treated and shot peened martensitic gear steels", *International Journal of Fatigue,* 31 (7) (2009) 1176-1189. https://doi.org/10.1016/j.ijfatigue.2008.12.001

[12] N. Salajegheh, R. Prasannavenkatesan, D. L. McDowell, G. B. Olson, and H.-J. Jou, "Finite element simulation of shielding/intensification effects of primary inclusion clusters in high strength steels under fatigue loading", 136 (2014) https://doi.org/10.1115/1.4027380]

[13] C. Hennessey, G. M. Castelluccio, and D. L. McDowell, "Sensitivity of polycrystal plasticity to slip system kinematic hardening laws for al 7075-t6", *Materials Science and Engineering: A,* 687 (2017) 241-248. https://doi.org/10.1016/j.msea.2017.01.070

[14] C. D. Hennessey, *Modeling microstructurally small crack growth in al 7075-t6*, Masters Thesis, George W. Woodruff School of Mechanical Engineering, Georgia Institute of Technology, (2015).

[15] K. Gall, M. F. Horstemeyer, B. W. Degner, D. L. McDowell, and J. Fan, "On the driving force for fatigue crack formation from inclusions and voids in a cast a356 aluminum alloy", *International Journal of Fracture,* 108 (3) (2001) 207-233. https://doi.org/10.1023/a:1011033304600

[16] Y. Xue, D. L. McDowell, M. Horstemeyer, M. H. Dale, and J. Jordon, "Microstructure-based multistage fatigue modeling of aluminum alloy 7075-t651", 74 (2007) 2810-2823. https://doi.org/10.1016/j.engfracmech.2006.12.031

[17] C. P. Przybyla and D. L. McDowell, "Simulated microstructure-sensitive extreme value probabilities for high cycle fatigue of duplex ti–6al–4v", *International Journal of Plasticity,* 27 (12) (2011) 1871-1895. https://doi.org/10.1016/j.ijplas.2011.01.006

[18] C. P. Przybyla and D. L. McDowell, "Microstructure-sensitive extreme-value probabilities of high-cycle fatigue for surface vs. Subsurface crack formation in duplex ti–6al–4v", *Acta Materialia,* 60 (1) (2012) 293-305. https://doi.org/10.1016/j.actamat.2011.09.031

[19] G. B. Olson, "Computational design of hierarchically structured materials", *Science,* 277 (5330) (1997) 1237-1242. https://doi.org/10.1126/science.277.5330.1237

[20] A. Goulding, J. F. Leung, and R. Neu, "Communicating materials systems knowledge through processing-structure-propertiesperformance (pspp) maps", *Journal of Materials Education,* 40 (1-2) (2018) 1-18.

[21] G. Lütjering and J. C. Williams, Beta alloys. Springer, 2007.

[22] M. A. Groeber and M. A. Jackson, "Dream.3d: A digital representation environment for the analysis of microstructure in 3d", *Integrating Materials and Manufacturing Innovation,*

3 (1) (2014) 1-17. https://doi.org/doi:10.1177/10567895990800406 10.1186/2193-9772-3-5

[23] M. Diehl, M. Groeber, C. Haase, D. A. Molodov, F. Roters, and D. Raabe, "Identifying structure–property relationships through dream.3d representative volume elements and damask crystal plasticity simulations: An integrated computational materials engineering approach", *JOM,* 69 (5) (2017) 848-855. https://doi.org/doi:10.1177/10567895990800406 10.1007/s11837-017-2303-0

[24] P. A. Shade, M. A. Groeber, J. C. Schuren, and M. D. Uchic, "Experimental measurement of surface strains and local lattice rotations combined with 3d microstructure reconstruction from deformed polycrystalline ensembles at the micro-scale", *Integrating Materials and Manufacturing Innovation,* 2 (1) (2013) 5. https://doi.org/10.1186/2193-9772-2-5

[25] S. D. Sintay, M. A. Groeber, and A. D. Rollett, "3d reconstruction of digital microstructures," in *Electron backscatter diffraction in materials science*, A. J. Schwartz, M. Kumar, B. L. Adams, and D. P. Field, Eds. Boston, MA: Springer US, 2009, pp. 139-153. https://doi.org/10.1007/978-0-387-88136-2_10

[26] T. Lacy, R. Talreja, and D. L. McDowell, Effects of damage distribution on evolution. 1997, pp. 131-149.

[27] D. L. McDowell, "Damage mechanics and metal fatigue: A discriminating perspective", *International Journal of Damage Mechanics,* 8 (4) (1999) 376-403. https://doi.org/doi:10.1177/105678959900800406

[28] T. Kanit, S. Forest, I. Galliet, V. Mounoury, and D. Jeulin, "Determination of the size of the representative volume element for random composites: Statistical and numerical approach", *International Journal of Solids and Structures,* 40 (13) (2003) 3647-3679. https://doi.org/10.1016/S0020-7683(03)00143-4

[29] S. M. Qidwai *et al.*, "Estimating the response of polycrystalline materials using sets of weighted statistical volume elements", *Acta Materialia,* 60 (13) (2012) 5284-5299. http://dx.doi.org/10.1016/j.actamat.2012.06.026

[30] M. Zhang, J. Zhang, and D. L. McDowell, "Microstructure-based crystal plasticity modeling of cyclic deformation of ti–6al–4v", *International Journal of Plasticity,* 23 (8) (2007) 1328-1348. http://doi.org/10.1016/j.ijplas.2006.11.009

[31] B. D. Smith, D. S. Shih, and D. L. McDowell, "Cyclic plasticity experiments and polycrystal plasticity modeling of three distinct ti alloy microstructures", *International Journal of Plasticity,* 101 (2018) 1-23. https://doi.org/10.1016/j.ijplas.2013.10.004

[32] J. R. Mayeur and D. L. McDowell, "A three-dimensional crystal plasticity model for duplex ti–6al–4v", *International Journal of Plasticity,* 23 (9) (2007) 1457-1485. http://doi.org/10.1016/j.ijplas.2006.11.006

[33] D. F. Socie and G. B. Marquis, Multiaxial fatigue. Society of Automotive Engineers Warrendale, PA, 2000.

[34] M. W. Brown and K. J. Miller, "A theory for fatigue failure under multiaxial stress-strain conditions", *Proceedings of the Institution of Mechanical Engineers,* 187 (1) (1973) 745-755. https://doi.org/10.1243/pime_proc_1973_187_069_02

[35] A. Fatemi and D. F. Socie, "A critical plane approach to multiaxial fatigue damage including out-of-phase loading", *Fatigue & Fracture of Engineering Materials & Structures,* 11 (3) (1988) 149-165. https://doi.org/10.1111/j.1460-2695.1988.tb01169.x

[36] D. L. McDowell, "Multiaxial fatigue strength," in *Fatigue and fracture*, A. S. M. H. Committee, Ed.: ASM International, 1996.

[37] D. L. McDowell and J.-Y. Berard, "A δj-based approach to biaxial fatigue", *Fatigue & Fracture of Engineering Materials & Structures,* 15 (8) (1992) 719-741. https://doi.org/doi:10.1111/j.1460-2695.1992.tb00053.x

[38] G. M. Castelluccio and D. L. McDowell, "Assessment of small fatigue crack growth driving forces in single crystals with and without slip bands", *International Journal of Fracture,* 176 (1) (2012) 49-64. https://doi.org/10.1007/s10704-012-9726-y

[39] A. Pineau, D. L. McDowell, E. P. Busso, and S. D. Antolovich, "Failure of metals ii: Fatigue", *Acta Materialia,* 107 (2016) 484-507. https://doi.org/10.1016/j.actamat.2015.05.050

[40] D. L. McDowell and F. P. E. Dunne, "Microstructure-sensitive computational modeling of fatigue crack formation", *International Journal of Fatigue,* 32 (9) (2010) 1521-1542. https://doi.org/10.1016/j.ijfatigue.2010.01.003

[41] G. M. Castelluccio and D. L. McDowell, "Mesoscale modeling of microstructurally small fatigue cracks in metallic polycrystals", *Materials Science and Engineering: A,* 598 (2014) 34-55. https://doi.org/10.1016/j.msea.2014.01.015

[42] C. J. Szczepanski, S. K. Jha, J. M. Larsen, and J. W. Jones, "Microstructural influences on very-high-cycle fatigue-crack initiation in ti-6246", *Metallurgical and Materials Transactions A,* 39 (12) (2008) 2841-2851. https://doi.org/10.1007/s11661-008-9633-z

[43] M. Peters, A. Gysler, and G. LÜtjering, "Influence of texture on fatigue properties of ti-6al-4v", *Metallurgical and Materials Transactions A,* 15 (8) (1984) 1597-1605. https://doi.org/10.1007/bf02657799

[44] G. Lütjering and J. C. Williams, Titanium. Springer, 2007.

[45] X. Du and W. Chen, "Efficient uncertainty analysis methods for multidisciplinary robust design", *AIAA Journal,* 40 (3) (2002) 545-552. https://doi.org/10.2514/2.1681

[46] M. McDonald and S. Mahadevan, "Uncertainty quantification and propagation in multidisciplinary analysis and optimization," in *12th aiaa/issmo multidisciplinary analysis and optimization conference*(Multidisciplinary analysis optimization conferences: American Institute of Aeronautics and Astronautics, 2008. https://doi.org/10.2514/6.2008-6038

[47] H.-J. Choi, D. L. McDowell, J. K. Allen, and F. Mistree, "An inductive design exploration method for hierarchical systems design under uncertainty", *Engineering Optimization,* 40 (4) (2008) 287-307. https://doi.org/10.1080/03052150701742201

[48] P. C. Kern, M. W. Priddy, B. D. Ellis, and D. L. McDowell, "Pydem: A generalized implementation of the inductive design exploration method", *Materials & Design,* 134 (Supplement C) (2017) 293-300. https://doi.org/10.1016/j.matdes.2017.08.042

[49] S. Roy, S. Suwas, S. Tamirisakandala, D. B. Miracle, and R. Srinivasan, "Development of solidification microstructure in boron-modified alloy ti–6al–4v–0.1b", *Acta Materialia,* 59 (14) (2011) 5494-5510. https://doi.org/10.1016/j.actamat.2011.05.023

[50] Y. C. Wang and T. G. Langdon, "Influence of phase volume fractions on the processing of a ti–6al–4v alloy by high-pressure torsion", *Materials Science and Engineering: A,* 559 (2013) 861-867. https://doi.org/10.1016/j.msea.2012.09.034

[51] N. Gey and M. Humbert, "Characterization of the variant selection occurring during the α→β→α phase transformations of a cold rolled titanium sheet", *Acta Materialia,* 50 (2) (2002) 277-287. https://doi.org/10.1016/S1359-6454(01)00351-2